



Numerical Modeling for the Solution of The Laser Heating by Using the Finite Element Method

**Dr.Mohammed
Mejbil saleh**

Associate Professor, Department of MBA, sreenivasa Institute Of Technology and Management Studies (SITAMS), Murakambattu (post), Chittoor-517127, Andhra Pradesh.

ABSTRACT

The laser beam can be used as a tool for the direct shaping or forming of metallic components by using the beam as a localized and highly controllable heat source. Laser thermal forming is achieved by inducing bending through the introduction of a steep thermal gradient into a sheet material or rod which results in local plastic deformation and subsequent shrinkage on cooling and heating process. In this paper we build a mathematical model to analyze the heating process by using laser beam. The model solved numerically by using the finite element method (FEM) in which the proposed model divided to (2254) elements to satisfy high accuracy of solution, a finite-element discretization to convert the PDEs to a set of nonlinear algebraic equations. The solutions obtained here employ the segregated solution algorithm, in which the equations are solved sequentially, as opposed to being assembled into a matrix equation and solved simultaneously. Since the equations are nonlinear and coupled, the segregated method requires that an iterative process be used. The results represented in 2d and 3d curves. From the model we obtained the boundary temperature distribution contours, normal heat flux, Temperature gradient curves and many other cases, the results give us good agreement with international published researches.

KEYWORDS

laser heating , laser technology

Introduction

A laser is defined as a device or instrument that emits electromagnetic radiation or light via an optical amplification process that is based on photons' stimulated emission. The temperature of a laser will depend on the type of laser used. The laser is used to heat the surface of materials. Any subsurface heating is accomplished by conduction. For intensity values up to about $1 \times 10^4 \text{ W/cm}^2$, the absorbed power depends on the wavelength, the material (and its surface condition). Generally, as the material temperature increases, so does the absorption of laser light. The most relevant processing parameters are the laser power and the beam/material interaction time. In metals, local surface heating is very rapid and produces a thin hot layer on a relatively cool bulk material. This conducts heat away from the surface very quickly. Cooling rates of the order of several thousand degrees per second are possible, which can be used to advantage in producing microstructural changes, for example, in transformation hardening which uses IR lasers.

Due to difficulties in the reproducibility of the energy output and distribution of the gas torch used and the fact of manual application, the quality of the result depends highly on the skill and experience of the workers. Different heat sources can be used to generate thermal stress in the material which can generate plastic deformation. Some of these sources are: gas torch, induction coil, electron beam, laser beam and plasma jet. The application of the laser beam for materials processing became more and more favorable [1, 2].

The laser beam has a flexibility with regard to processing parameters which is nearly as high as for the electron beam, but without the need of a vacuum. The energy transferred into the specimen by a laser beam can be controlled very precisely, if necessary by a closed-loop control, which guarantees a very high reproducibility. The development of new generations of lasers enabled new processes to be economical. The high power CO_2 , diode, fibre and disc lasers became efficient heat sources for the processing of larger parts, whereas increasing beam quality enables very small laser spots on the surface of the part to be achieved and therefore enables the processing of small parts [3].

Actually, modeling and simulation relevant to developing im-

proved technical applications improved by extending the scientific basis from macro applications into the field of shorter pulses of about a few nano-seconds and smaller length scales down to the wavelength of the radiation is considered. Some key physical phenomena become apparent and more dominant on smaller scales. As a result, there is also feedback from improved models on the micro-scale to simulations describing macro-applications. The analysis deals with the interaction of physical quantities including photon and wave properties of radiation, energy flow density and photon energy [4, 5].

Theoretical basis

Examples might be thermal energy, particles diffusing through some medium, or a contaminating chemical. If it has a concentration C and Q is conserved, then its flow rate q_c is related to C by Fick's First Law,

$$q_c = -D \nabla C \dots \dots \dots (1)$$

relative to the underlying medium, which is normally assumed to be at rest. For a true conservation condition, G^*_{*i} and q^* are both identically zero. Mathematically, the generalized conservation statement can be written

$$\frac{d}{dt} \int_V k_* dV = \int_V q_* dV - \int_S Q_{*j} n_j dS + \int_S G_{*j} n_j dS \dots \dots \dots (2)$$

Eq.2 has the equivalent mathematical form

$$\frac{\partial k_*}{\partial t} + \frac{\partial Q_{*j}}{\partial x_j} = q_* + \frac{\partial G_{*j}}{\partial x_j} \dots \dots \dots (3)$$

Suppose Q is defined at every point in some region of space V contained within the domain of investigation D , and that there is a density k_* units of Q per unit volume at each point of V , where k_* is a tensor of order $r \geq 0$ with $*$ indicating an appropriate set of r subscripts;

- there is a flow Q_i defined at each point of D so that the direction of flow and magnitude of the quantity whose density is measured by k_i is Q_i units of Q per unit area per unit time;
- at an element with an outward unit normal n of the surface S of V , there is a rate of generation $G_j n_j$ units of Q per unit area of S per unit time.
- a net number q_v units of Q are generated per unit volume per unit time.

In eq. 1 D is a diffusion coefficient. Conservation of Q , by eq. 3, in the absence of any generation processes, gives

$$\frac{\partial C}{\partial t} + \nabla \cdot q_c \dots \dots \dots (4)$$

If this equation is combined with eq. 1, Fick's Second Law is obtained,

Provided the diffusion constant D can be regarded as a constant [6]. The metallurgy of a laser processed material is strongly governed by local diffusion processes that in turn are driven by thermal and chemical gradients. The diffusion mechanism and the concentration distribution $c(x, y, z; t)$ to be calculated is basically described by Fick's first and second laws as shown during eq. 1 and 2 respectively. The diffusion constant C is basically a measure for the mobility of a certain chemical element in some different atomic environment, e.g. in a crystal lattice or in a liquid of a different element. The diffusion constant D can depend strongly on the temperature [7].

Results and discussion

High contrast of temperature distribution of the laser heating model shown in figure. 1, and during this contour the model has two symmetrical sides. The first side shadow, the other side bright and flash arrow appear at the middle of the model.

High temperature 515.68 K concentrated at the middle as shown in the graded colored bar beside figure. 1, and from this bar the minimum temperature 300 K exists at the shadow side and at the base of the model.

Curves of temperature distribution versus length of the model shown in the figure. 2, and during this figure the temperature alternative distributed around 0.02 length. On this length, the temperature increase in to high value then decrease with increase length of the model.

Low brightness of the flash arrow emerged at the middle point of the model during contour of normal heat flux as shown in figure. 3. Maximum value of heat flux extremely higher than 8×10^5 w/m² shown in figure.4 during curves of heat flux.

These curves have some different behavior than that appear in curves of temperature distribution. In this context, these curves match with previously behavior of temperature distribution, where high value of heat flux occur on the 0.02 length of the laser heating model.

Temperature gradient curves shown in figure.5, display uniform and homogeneous distributed of temperature gradient. At the intervals from 0.015 to 0.025 length of the model, the values of temperature gradient increase from extremely zero to 0.6×10^4 , 1.2×10^4 and 2×10^4 K/m respectively on the 0.02 length of the model then from this point the values repeated to the zero.

Conclusion

Laser heating model emerged two symmetrical sides of temperature distribution. The first side shadow while the other side bright. Maximum temperature 515.68 K concentrated at the middle and the minimum temperature 300 K exists at the shadow side and at the base of the model.

Some behavior of heat flux incompatible with temperature

distribution where temperature alternative distributed. Temperature gradient homogeneous distributed at the intervals from 0.015 to 0.025 length of the model.

On the 0.02 length of the model, the maximum value of heat flux extremely higher than 8×10^5 w/m² and temperature gradient explosively increase from extremely zero to 2×10^4 K/m then repeated to the zero.

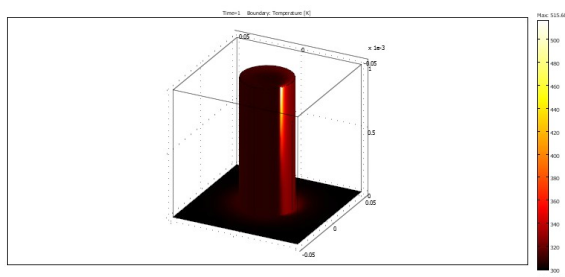


Figure. 1: Temperature distribution contour

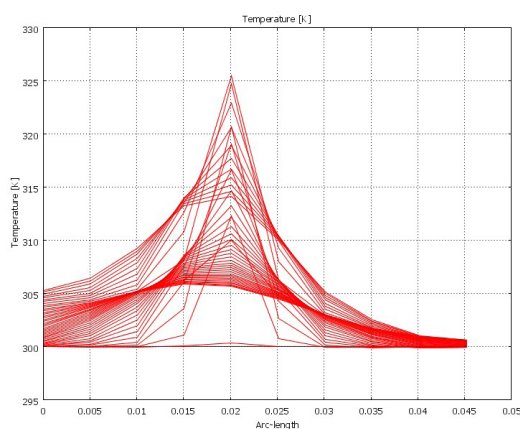


Figure. 2: Curve of temperature distribution

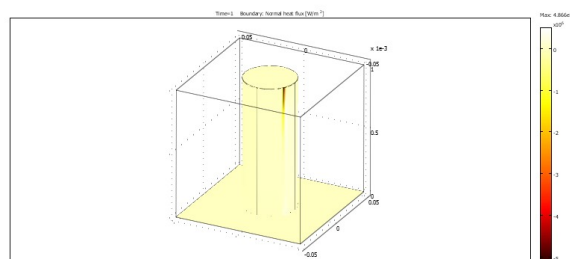


Figure. 3: Normal heat flux

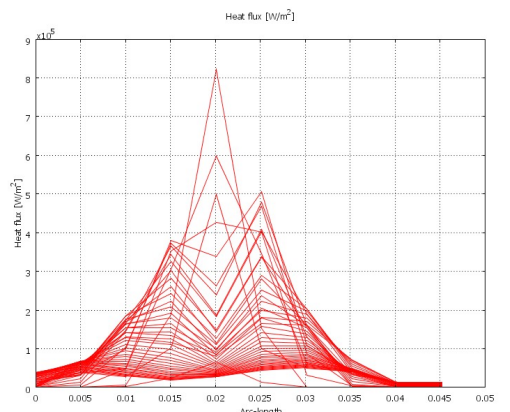


Figure. 4: curves of heat flux

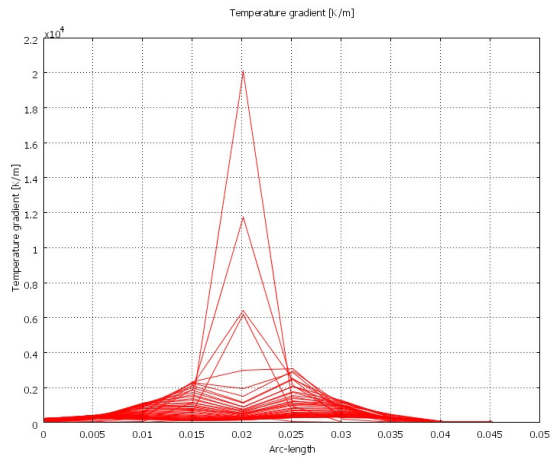


Figure. 5: Temperature gradient curves

REFERENCES

1. Namba Y (1985) Laser Forming in Space. In: Proc. Lases'85 403–407. | 2. Namba Y (1987) Laser Forming of Metals and Alloys. In: Laser Advanced | Materials Processing LAMP'87, High Temp. Soc. of Japan and Japan Laser | Processing Soc 601–606. | 3. Uelze A (1988) Thermisches Richtpunkten von gebeulten Feinblechfeldern. | Schweitechnik, vol 38 no 4, Berlin-Ost 166–168. | 4. Horn A, Mingareev I, Miyamoto I (2006) Ultra-fast diagnostics of laser-induced melting of matter. JLMN-Journal of Laser Micro/Nano engineering 1(3): 264–268. | 5. Horn A, Mingareev I, Werth A, Kachel M, Brenk U (2007) Investigations on ultrafast welding of glass-glass and glass-silicon. 9th International Conference on Laser Ablation, Tenerife (Spain) 24–28 September 2007, in press. | 6. Spitzer L (1962) Physics of fully ionized gases. Inter science, New York. | 7. Lampa C, Kaplan AFH, Powell J, Magnusson C (1997) Fluid flow and re solidification in deep penetration laser welding. Lasers in Engineering 7: 241–252. |